

This site uses cookies. By continuing to use this site you agree to our use of cookies. To find out more, see our [Privacy and Cookies](#) policy. ☐



RNAAS RESEARCH NOTES OF THE AAS



A publishing partnership

New Tools for Self-consistent Modeling of the AGN Torus and Corona

Mislav Baloković^{1,2}, Javier A. García^{3,4}, and Samantha E. Cabral^{1,2,5}

Published 2019 November 15 • © 2019. The American Astronomical Society. All rights reserved.

[Research Notes of the AAS](#), [Volume 3](#), [Number 11](#)

[Get permission to re-use this article](#)

Share this article



☐ Article information

Export citation and abstract

[BibTeX](#)

[RIS](#)

[Footnotes](#)

[References](#)

The continuum emission typically observed in the X-ray spectra of active galactic nuclei (AGNs) is thought to arise from inverse-Compton scattering of blackbody photons from the accretion disk by mildly relativistic thermal electrons in a rarefied and relatively hotter corona. By fitting theoretical spectral models (e.g., Poutanen & Svensson [1996](#); Coppi [1999](#)) to the observed shape of an AGN coronal continuum it is possible to constrain some of its physical parameters, such as the electron temperature and optical depth (e.g., Fabian et al. [2015](#); Middei et al. [2019](#)).

X-ray reprocessing (Compton scattering, absorption, and fluorescence)

adds spectral features that make it possible to constrain properties of the material surrounding the innermost parts of an AGN, such as its covering factor and its average—as opposed to line-of-sight—column density (Baloković et al. 2018; B18 hereafter). Models with complex torus-like reprocessing geometries that have recently been discussed in the literature (e.g., Buchner et al. 2019; Tanimoto et al. 2019) approximate the coronal continuum as a power law with either an exponential cutoff () or a sharp termination at a certain energy. The reprocessed spectrum is formed by down-scattering of this high-energy emission, making it important to consider more realistic coronal spectra.

Hereby we publicly release new spectral template libraries in tabulated form convenient for analysis of X-ray data, extending the BORUS suite of models first described in B18. They are standard-format FITS tables readable in the spectral fitting tool XSPEC (Arnaud 1996). The new model tables, `borus11` and `borus12`, are equivalents of older versions `borus01` and `borus02` regarding geometry, uniform density, and radiative transfer calculations. However, the phenomenological power law with an exponential cutoff is replaced with the Comptonized continuum based on the `nthcomp` model (Zdziarski et al. 1996; Życki et al. 1999) as implemented in XSPEC.⁶

`borus11` features a spherical reprocessor geometry and has 6 parameters: photon index (Γ [1.4, 2.6]), coronal temperature (kT_e/keV [5, 500]; instead of the high-energy cutoff, E_{cut} , in the older versions), column density of the torus ($\log N_{\text{H,tor}}/\text{cm}^{-2}$ [22.0, 25.5]), relative iron abundance in the torus (A_{Fe} [0.1, 10]), redshift, and normalization of the intrinsic continuum. The geometry assumed for `borus12` is a sphere with polar conical cut-outs defined with two additional parameters: torus covering factor (C_{tor} [0.1, 1.0]) and inclination ($\cos \theta_{\text{inc}}$ [0.05, 0.95]). The `nthcomp` input spectrum has a disk-like blackbody seed photon distribution with a temperature of 0.05 keV.

The new XSPEC-format tables are publicly available on the Web.⁷ The download page provides examples of complete XSPEC models that can be used to simultaneously constrain torus parameters and kT_e by fitting broadband X-ray data of sufficient quality. They can also be self-consistently incorporated into complex spectral models with relativistic reprocessing component represented by versions of the `relxill` model (Dauser et al. 2014; García et al. 2014) that use the same Comptonized

continuum,⁸ albeit with differently defined continuum normalization (Dauser et al. 2016).

To demonstrate the applicability of the new model tables, we select the bright nearby type-II Seyfert NGC 5506, for which *NuSTAR* and *Swift*/XRT spectra have previously been modeled by Matt et al. (2015) and Tortosa et al. (2018) with the aim of constraining kT_e . For simplicity, we make use of the same data and refer to the previous work for technical details. We bin the spectra using a custom-built script described in Baloković (2017).

Our spectral model is defined with the XSPEC expression

`const × phabs × (zphabs × cabs × (nthcomp + relxillCp) + atable{borus12})`,

representing the cross-normalization factor, Galactic absorption, AGN-related absorption, coronal continuum, relativistic reprocessing, and torus reprocessing, respectively. We link Γ , kT_e , and normalization parameters of the additive components. The `relxillCp` component has the `rel_refl` parameter fixed at -1 and free normalization. We fix its other parameters following a detailed multi-epoch study by Sun et al. (2018), and assume Solar iron abundance and an inclination of 40° . An in-depth discussion of other potential choices is left for a future publication.

This model fits the data well ($\chi^2/\nu = 612.5/559$), yielding , where ν is the number of degrees of freedom and the uncertainty spans the 68% confidence interval. While removing the relativistic component slightly increases the χ^2 , further including a narrow line corresponding to ionized iron ($E_{\text{line}} = 6.86 \pm 0.06$ keV) results in a decrease ($\chi^2/\nu = 606.8/558$). The kT_e constraint then appears tighter, , demonstrating how the choice of model details can influence constraints. In Figure 1 we show two-dimensional constraints for the torus and corona parameters. With or without the relativistic component, the torus parameters ($C_{\text{tor}} \approx 0.75$, $\log N_{\text{H,tor}}/\text{cm}^{-2} \approx 24.8$) fall in between those presented in B18, adding to the observed diversity of torus properties.

☐ Zoom In ☐ Zoom Out ☐ Reset image size

Figure 1. Two-dimensional constraints on torus and corona parameters for NGC 5506 based on spectral fitting of *NuSTAR* and *Swift*/XRT spectra. Contours show 1, 2, and 3 σ constraints going from darker to lighter colors, and the white \times markers show the best-fit values. Note

that in the first model (left pair of panels, green contours) the 1σ constraint on kT_e scales with $\log N_{\text{H,tor}}$, while in the second model (right pair, blue contours) it appears independent.

Download figure:

☐ Standard image

☐ High-resolution image



☐ Export PowerPoint slide












We acknowledge support from the black hole Initiative at Harvard University, funded by the John Templeton Foundation and the Gordon and Betty Moore Foundation (grant GBMF8273). This work was also supported by the Alexander von Humboldt Foundation and *Chandra* Theory grants TM8-19003X (J.A.G.) and TM9-20004X (M.B.).

Footnotes

- 6 <https://heasarc.gsfc.nasa.gov/xanadu/xspec/manual/node203.html>
- 7 <http://www.astro.caltech.edu/~mislavb/download>
(alternatively, <https://doi.org/10.5281/zenodo.3538232>)
- 8 <http://www.sternwarte.uni-erlangen.de/~dauser/research/relxill/index.html>

References

- ☐ Arnaud K. A. 1996 *ASP Conf. Ser. 101, Astronomical Data Analysis Software and Systems V* ed G. H. Jacoby and J. Barnes (San Francisco, CA: ASP) 17
[ADS](#) [Google Scholar](#) - 
- ☐ Baloković M. 2017 *PhD thesis* California Institute of Technology
doi:[10.7907/Z9WM1BG8](https://doi.org/10.7907/Z9WM1BG8)
[ADS](#) [Google Scholar](#) - 
- ☐ Baloković M., Brightman M., Harrison F. A. *et al* 2018 *ApJ* **854** 42
[IOPscience](#) [ADS](#) [Google Scholar](#) - 
- ☐ Buchner J., Brightman M., Nandra K., Nikutta R. and Bauer F. E. 2019 *A&A* **629** A16
[Crossref](#) [ADS](#) [Google Scholar](#) - 

- [□](#) Coppi P. S. 1999 *ASP Conf. Ser. 161, High Energy Processes in Accreting Black Holes* ed J. Poutanen and R. Svensson (San Francisco, CA: ASP) 375 arXiv:astro-ph/9903158
[ADS](#) [Preprint](#) [Google Scholar](#) - 
- [□](#) Dauser T., Garcia J., Parker M. L., Fabian A. C. and Wilms J. 2014 *MNRAS* **444** L100
[Crossref](#) [ADS](#) [Google Scholar](#) - 
- [□](#) Dauser T., García J., Walton D. J. *et al* 2016 *A&A* **590** A76
[Crossref](#) [ADS](#) [Google Scholar](#) - 
- [□](#) Fabian A. C., Lohfink A., Kara E. *et al* 2015 *MNRAS* **451** 4375
[Crossref](#) [ADS](#) [Google Scholar](#) - 
- [□](#) García J., Dauser T., Lohfink A. *et al* 2014 *ApJ* **782** 76
[IOPscience](#) [ADS](#) [Google Scholar](#) - 
- [□](#) Matt G., Baloković M., Marinucci A. *et al* 2015 *MNRAS* **447** 3029
[Crossref](#) [ADS](#) [Google Scholar](#) - 
- [□](#) Middei R., Bianchi S., Marinucci A. *et al* 2019 *A&A* **630** A131
[Crossref](#) [ADS](#) [Google Scholar](#) - 
- [□](#) Poutanen J. and Svensson R. 1996 *ApJ* **470** 249
[Crossref](#) [ADS](#) [Google Scholar](#) - 
- [□](#) Sun S., Guainazzi M., Ni Q. *et al* 2018 *MNRAS* **478** 1900
[Crossref](#) [ADS](#) [Google Scholar](#) - 
- [□](#) Tanimoto A., Ueda Y., Odaka H. *et al* 2019 *ApJ* **877** 95
[IOPscience](#) [ADS](#) [Google Scholar](#) - 
- [□](#) Tortosa A., Bianchi S., Marinucci A., Matt G. and Petrucci P. O. 2018 *A&A* **614** A37
[Crossref](#) [ADS](#) [Google Scholar](#) - 
- [□](#) Zdziarski A. A., Johnson W. N. and Magdziarz P. 1996 *MNRAS* **283** 19

[Crossref](#)

[ADS](#)

[Google Scholar](#)



 Życki P. T., Done C. and Smith D. A. 1999 *MNRAS* **309** 561

[Crossref](#)

[ADS](#)

[Google Scholar](#)




Export references:

[BibTeX](#)

[RIS](#)

[Journals](#) [Books](#) [About IOPscience](#) [Contact us](#) [Developing countries access](#)

[IOP Publishing open access policy](#)

© Copyright 2019 IOP Publishing [Terms & conditions](#) [Disclaimer](#) [Privacy & cookie policy](#) 

This site uses cookies. By continuing to use this site you agree to our use of cookies.